Werk

Jahr: 1980
Kollektion: fid.geo
Signatur: 8 Z NAT 2148:47
Digitalisiert: Niedersächsische Staats- und Universitätsbibliothek Göttingen
Werk Id: PPN1015067948_0047
PURL: http://resolver.sub.uni-goettingen.de/purl?PPN1015067948_0047

LOG Id: LOG_0042
LOG Titel: Crustal development of the Reykjanes Ridge from seismic refraction
LOG Typ: article

Übergeordnetes Werk

Werk Id: PPN1015067948
PURL: http://resolver.sub.uni-goettingen.de/purl?PPN1015067948
OPAC: http://opac.sub.uni-goettingen.de/DB=1/PPN?PPN=1015067948

Contact

Niedersächsische Staats- und Universitätsbibliothek Göttingen
Georg-August-Universität Göttingen
Platz der Göttinger Sieben 1
37073 Göttingen
Germany
Email: gdz@sub.uni-goettingen.de

J. Geophys. 47, 261–264, 1980

Journal of Geophysics

Crustal Development of the Reykjanes Ridge From Seismic Refraction

A.W.H. Bunch
Department of Goedesy and Geophysics, Madingley Rise, Madingley Road, Cambridge CB3 OEZ, England

Abstract. A seismic refraction experiment was carried out on the Reykjanes Ridge at approximately 60° N 30° W to determine the detailed seismic structure of the crust and the way in which this structure changes with age. Three 120-km-long overlapping split reversed profiles were shot over crust of ages 0, 3, and 9 Ma on the Eastern flank of the ridge. The data gathered were first analysed using travel-time analysis, these structures were then refined by modelling the experimental waveforms with synthetic seismograms. The detailed structures obtained indicate that with increasing age the 4.6 km/s layer thins and the crust with velocities 6.6 to 7.1 km/s thickens and increases its mean velocity. The velocity of the deepest layer seen increases with age, 7.1 km/s at 0 Ma and 8.2 km/s at 9 Ma, the vertical transition to this velocity being modelled best by a velocity gradient (0.66 km/s/km).

Key words: Reykjanes ridge – Crustal ageing – Mid Atlantic Ridge – Seismic refraction.

Introduction

During the summer of 1977 Cambridge University carried out a seismic experiment on the Reykjanes Ridge, at approximately 60° N 30° W, (Fig. 1), the position chosen marks the south-western limit of the section of the Reykjanes Ridge with no median valley and at this latitude the ridge breaks up into sections whose axes lie obliquely to the overall spreading axis of the ridge (Shih et al., 1978). The Reykjanes Ridge north-east of 59° 30′ N also exhibits a lower level of seismicity, less than a quarter of the activity of the ridge further south-west (Francis, 1973).

The experiment was designed with two aims:

(i) To determine a detailed crustal structure for this section of the ridge.

(ii) To investigate the way in which the seismic crustal structure changes with age.

Three refraction lines were shot parallel to the ridge axis over crust of approximate ages 0, 3, and 9 Ma, these ages corresponding to the crest of the ridge, the foot of the central triangular section of the ridge, and the edge of a raised plateau bordering the ridge. The lines shot were 120 km long 'overlapping-split reserved' profiles with a maximum shot receiver range of 70 km. On each line between four and five receivers (free floating recording sonobuoys) were used and up to 33 shots detonated. In addition, to determine the sediment thickness, normal incidence reflection profiles were shot, using a Geomechanique array, over the 3 and 9 Ma refraction lines, but none over the ridge axis, as previous work (Ruddiman, 1972) indicated that there was no sedimentary cover.

Travel-Time Analysis

Good quality amplitude data were obtained from all the shots at all the receivers. The first arrival times were picked from unfiltered digital record sections, the correlations being facilitated by using filtered record sections. The arrival times were corrected for the varying sedimentary thicknesses and water depths below shot and receivers. The timing corrections made for variations in the water depth were calculated assuming that all sub-basement interfaces lay parallel to the basement topography (Kennett and Orcutt, 1976). This assumption is common for marine refraction work and is usually justified in areas where the basement relief exhibits only gentle undulations, as on the 0 and 9 Ma profiles. On the 3 Ma profile the basement topography was rough and any assumption, when calculating the water depth correction, would be hard to justify for the data collected. An alternative assumption would be that all the basement topography was due to variations in thickness of the shallowest seismic layer, all sub-

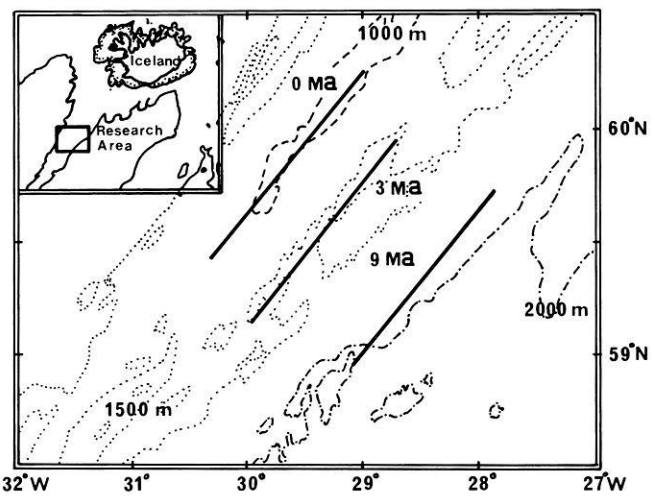

Fig. 1. Chart showing location of the three refraction profiles (*solid lines*) described in the text. The profiles were shot over crust of approximate ages 0, 3, and 9 Ma. Contours at 500 m intervals are given (Shih et al., 1978). The position of the research area relative to Iceland is shown in the *inset*

0340-062X/80/0047/0261/$01.00

basement interfaces being flat. These two different approaches in calculating the water depth correction give rise to differences of 0.040 s for the timing corrections of the data gathered, this error being of the same magnitude as the errors on the arrival time data in the travel-time analysis. However, no correlation was found between these travel-time errors and the calculated water depth corrections which suggests that the assumption used was appropriate.

The arrival times from all the sonobuoys could be combined from both the 0 and 9 Ma profiles giving a high data density. On the 3 Ma line poor control on the water depth below four of the five sonobuoys made it necessary to determine time delays which would make it possible to overlay the arrival times. For each profile the combined arrivals were then split into groups, each representing one 'refractor'. An indication of the ranges at which to split the data was found by examining the behaviour with range of:

(i) The waveform of the first arrival wave-group (taking into account change due to variations of shot size).

(ii) The peak to peak amplitude of the first arrival wave-group.

The shape and amplitude of the first arrival wave-packet showed marked changes over a narrow range band, e.g., at 25 km for the 0 Ma profile Fig. 3 and 4. These ranges, 'cross-over' ranges, were taken as indicating a change in the nature of the seismic arrivals as the changes could not be accounted for by variations of shot size. Using these 'cross-over' ranges as a guide, the arrivals were assigned to the various groups, the arrivals coming from ranges near to, less than 5 km, the 'cross-over' ranges being assigned to groups with the aid of time-distance plots of all the arrivals. Least-squares lines were fitted to the data groups and from the results the structures shown in Fig. 2 were calculated.

The velocity-depth bounds shown in Fig. 2 were derived from the 'tau' technique of Bessonova et al. (1974) with the modifications of Kennett and Orcutt (1976). The first arrival groups gave only a patchy tau-p curve which was completed using the method of parallelograms (Keilis-Borok, 1971). The completed bounds were then inverted into velocity-depth bounds using the Herglotz-Wiechert integral. On the 3 Ma profile, due to the poor quality data, the arrivals were not divided up into groups when forming the tau-p curve. Thus the velocity-depth bounds for this profile are broader and show less structure. The velocity-depth bounds found from the 'tau' technique are useful in that they give a guide for alterations to the first arrival structure when matching the amplitude-distance behavior of seismograms.

Surface Structure

The structure of the top 2 km of the crust was determined from data gathered when recovering the sonobuoys using a 1,000 in.^{3} air-gun as sound source. In addition to the refraction data gathered in this way, wide angle reflections were seen coming from an interface below the basement. On all three profiles these reflections were interpreted as coming from the base of the layer with velocity 4.6 km/s. These reflections were only seen over a narrow range window, the amplitude rising and falling sharply. This amplitude-distance behavior (Červený and Zahrandnik, 1972) suggests that a velocity gradient underlies the 4.6 km/s layer. On the 3 Ma line, where the data density was highest, the seismic structure from the travel-time data modelled the crust at the base of the 4.6 km/s layer with thin layers, this being an equivalent representation of a velocity gradient in terms of constant velocity layers.

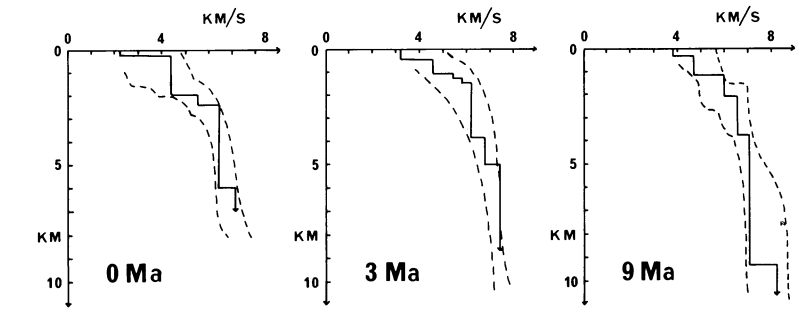

Fig. 2. The seismic velocity-depth structures (*solid lines*) calculated from the travel-times measured for the three refraction profiles. The *broken lines* are the velocity-depth bounds as calculated from the 'tau' technique (Bessonova et al., 1974)

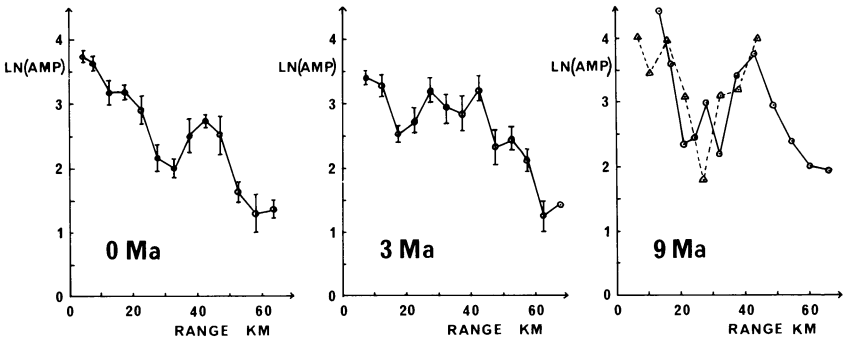

Fig. 3. Average amplitude-distance curves for the three refraction profiles. The amplitude is the peak to peak amplitude of the first arrival wave-group, the scale being arbitary. For the 0 and 3 Ma profiles the data from all buoys have been combined and averaged over 5 km range bins. The mean amplitude of each range bin is plotted together with the standard error in the mean. At both ends of the 3 Ma line the four shots furthest from the receivers gave anomalously low amplitudes, either due to lateral crustal variations or incomplete charge detonation. In this figure these amplitudes have been corrected for the latter effect. For the 9 Ma profile the results from only one sonobuoy are plotted, as the data from the other buoys were either noisy or incomplete. The *solid line* is for the section of the profile shot from the SW into the buoy and the *broken line* corresponds to shots NE of the buoys

Amplitude and Waveform Analysis

In order to define the general characteristics common to record-sections from all of the sonobuoys for a profile, average amplitude-distance curves were calculated for each profile. The amplitude plotted in Fig. 3 is the peak to peak amplitude of the first arrival wave-group. It can be seen that at certain ranges there are marked changes of amplitude and the position and magnitude of these changes were used as a descriminant when modelling the experimental records with synthetic seismograms.

All the modelling of the seismic record sections was completed using the reflectivity method (Fuchs and Müller, 1971; Kennett, 1975). For each profile, a synthetic record section was first computed for the travel-time structure. This structure was then altered by the addition of new layers in an attempt to improve the match of the amplitude behaviour between the synthetic and experimental record-sections. The changes in the velocity-depth structure were made so as to maintain the intercept times of the refractors seen as first arrivals.

On the 0 Ma line the travel-time velocity-depth structure was altered mainly by changes in the structure below 3.5 km depth. Layers of velocities 6.8, 6.6, and 6.8 km/s were included to increase the amplitude present at less than 25 km range and produce the correct drop in amplitude at 25 km (Fig. 3). The low-velocity zone was required to achieve the correct range to the amplitude peak at around 40 km. To increase the sharpness of this amplitude peak the 7.1 km/s interface was exchanged for a velocity gradient of 0.6 km/s/km. A comparison of the experimental and synthetic record sections is made in Fig. 4.

Two changes were made to the travel-time structure for the 9 Ma profile. The first alteration was the inclusion of a 6.9 km/s layer above the 7.1 km/s layer. This layer was included to increase the amplitude at less than 17 km range and decrease the amplitude at 25 km. The amplitude contrast was further improved by exchanging the 6.6 to 6.9 km/s interface to a velocity gradient. The second modification was to change the 7.1 to 8.2 km/s interface to a 0.66 km/s/km velocity gradient. This sharpened the amplitude peak of the synthetic seismograms at 40 km range, as seen on the experimental records (Fig. 5).

The data from the 3 Ma profile were of a poorer quality and thus the final structure obtained is not as well controlled as for the 0 and 9 Ma profiles. Anomalously low amplitudes on both ends of the profile from the four charges most distant from the receivers make it difficult to define the velocity structure below 6.5 km depth. However changes were made in the travel-time velocity-depth model to improve the match between the experimental and synthetic record sections of which the best solution is shown in Fig. 6.

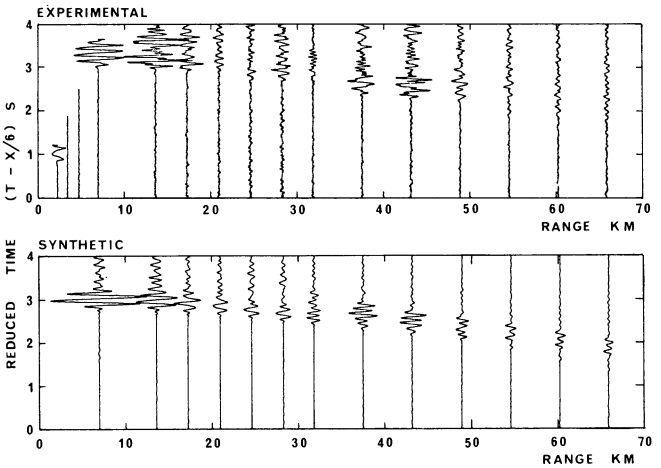

Fig. 5. Synthetic seismograms calculated for the final velocity depth structure proposed for the 9 Ma profile together with some of the experimental data. The experimental records have been scaled for range and varying charge weights, the same scaling for range being applied to the synthetic records

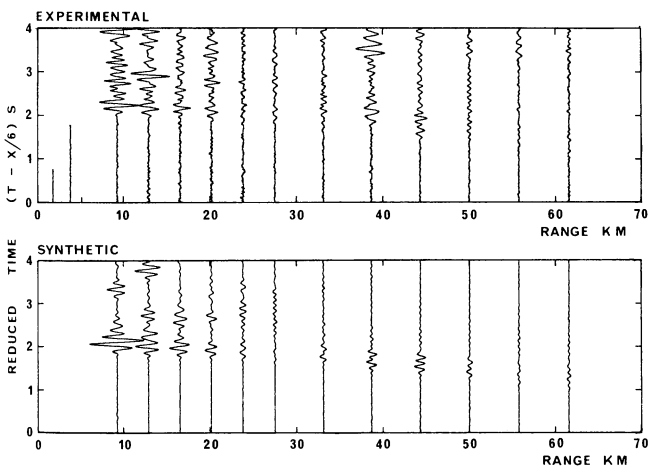

Fig. 4. Synthetic seismograms for the final velocity-depth structure proposed for the 0 Ma profile together with some of the experimental data. The experimental seismograms have been scaled for range and varying charge weight, the same scaling for range being used for the synthetic records. The energy delayed approximately 1 s from the first arrival corresponds to the sea-water multiple

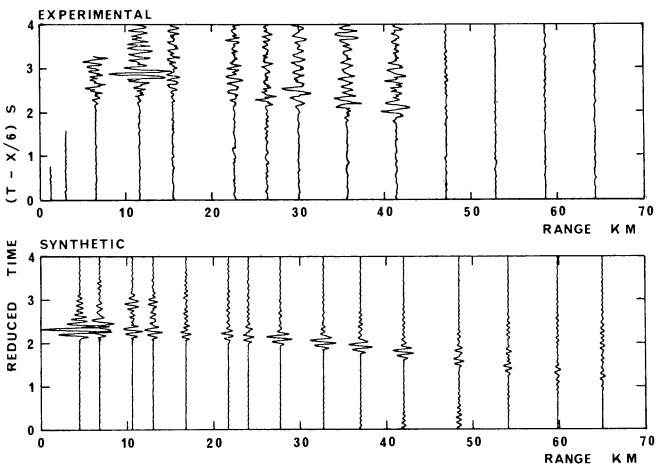

Fig. 6. Synthetic seismograms for the final velocity-depth structure proposed for the 3 Ma profile together with some of the experimental data. The experimental records have been scaled for range and varying charge weights, the same scaling for range being applied to the synthetic records. The anomolously low amplitudes beyond 45 km range may be due either to lateral changes in the crust along the profile or incomplete shot detonation. The amplitudes shown are scaled as if these shots fired completely

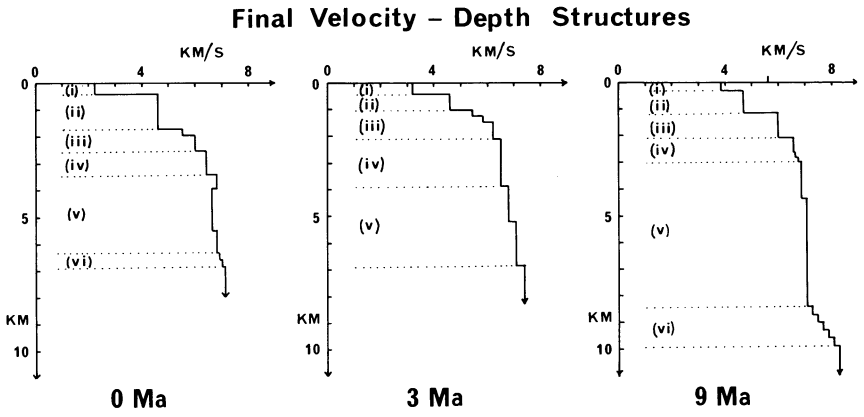

Fig. 7. The final velocity-depth structures proposed for the three refraction profiles. The Roman numerals correspond to the sections of the conclusions

Conclusions

The final velocity depth structures obtained for the three refraction profiles are shown in Fig. 7. Several conclusions may be made about the change in seismic structure with age. The trends with increasing age are:

(i) The sea-floor refraction velocity increases from 2.2 km/s at the ridge axis to 3.8 km/s for crust 9 Ma, these velocities being obtained from the air-gun observations.

(ii) The 4.6 to 4.7 km/s layer thins by 0.5 km in 9 Ma, but its velocity remains relatively constant.

(iii) The 5.4 to 6.2 km/s layers become shallower, though their combined thickness and mean velocity remain relatively constant. Wide-angle reflections from the base of the 4.6 km/s layer would indicate that this is a region of a velocity gradient rather than a constant velocity layer.

(iv) The 6.4 to 6.6 km/s layer also becomes shallower and its thickness appears relatively constant.

(v) The layers with velocities between 6.6 and 7.2 km/s increase their mean velocity and thickness. At the ridge axis a slight low velocity zone is present, velocity 6.6 km/s, below a 6.8 km/s lid. Away from the ridge the velocity increases and at 9 Ma this region has a mild velocity increase with depth.

(vi) The transition to the highest velocity measured is best modelled by a velocity gradient rather than a first-order discontinuity, the velocity gradient being approximately 0.66 km/s/km.

The structures obtained are relatively smooth structures. This suggests that the seismic model of the oceanic crust should be seen more as a smooth velocity-depth profile with changing velocity gradients rather than as a model of constant-velocity layers.

A more detailed discussion of the analysis and conclusions from this experiment may be found in Bunch and Kennett (1979).

Acknowledgements. I should like to thank the Master and crew of RRS Shackleton and everybody who helped at sea. T.J.G. Francis and the members of Blacknest aboard were of great help in carrying out the experiment. A. Claydon, M. Mason and R. Theobald were very helpful in building and maintaining the equipment used. I also thank C.M.R. Fowler, B.L.N. Kennett, K.E. Louden, and D.H. Matthews for their help in the experiment and in discussions of its analysis. This work was supported by a Shell studentship and by a NERC grant GR/3/1651.

References

Bessonova, E.N., Fishman, V.M., Ryaboyi, V.Z., Sitnikova, G.A.: The Tau method for inversion of travel-times – I. Deep seismic sounding data. Geophys. J. R. Astron. Soc. **36**, 377–398, 1974

Bunch, A.W.H., Kennett, B.L.N.: The crustal structure of the Reykjanes Ridge at 59° 30′ N. Geophys. J. R. Astron. Soc. in press, 1979

Červený, V., Zahrandnik, J.: Amplitude-Distance curves of seismic body waves in the neighbourhood of critical points and caustics – a comparison. Z. Geophys. **38**, 499–516, 1972

Francis, T.J.G.: The seismicity of the Reykjanes Ridge. Earth Planet. Sci. Lett. **18**, 119–123, 1973

Fuchs, K., Müller, G.: Computation of synthetic seismograms with the reflectivity method and comparison with observations. Geophys. J. R. Astron. Soc. **23**, 417–433, 1971

Keilis-Borok, V.J.: The inverse problem of seismology. In: Proceedings of the International School of Physics 'Enrico Fermi', course L, Mantle and Core in Planetary Physics, J. Coulomb and M. Caputo, eds.: pp. 242–274. New York: Academic Press, 1971

Kennett, B.L.N.: The effects of attenuation on seismograms. Bull. Seismol. Soc. Am. **65**, 1643–1651, 1975

Kennett, B.L.N., Orcutt, J.A.: A comparison of travel-time inversions for marine refraction profiles. J. Geophys. Res. **81**, 4061–4070, 1976

Ruddiman, W.F.: Sediment redistribution on the Reykjanes ridge: Seismic evidence. Bull. Geol. Soc. Am. **83**, 2039–2062, 1972

Shih, J.S.F., Atwater, T., McNutt, M.: A near-bottom geophysical traverse of the Reykjanes Ridge. Earth Planet. Sci. Lett. **39**, 75–83, 1978

Received April 6, 1979; Revised Version July 16, 1979